ORIGINAL RESEARCH PAPER

Fabrication and Charge Modification of Ceramic Membranes Using Copper Nanoparticles for Desalination

Majid Shokri Doodeji [1], Mohammad Mahdi Zerafat [1]*, Omid Nejadian

[1] *Faculty of Advanced Technologies, Nano Chemical Engineering Department, Shiraz University, Shiraz, Iran*

Received: 2017-08-25 Accepted: 2017-10-29 Published: 2017-12-01

ABSTRACT

Ceramic membranes are considered as alternatives for their polymeric counterparts due to high mechanical strength and thermal resistance; thus long lifetime. Usually, asymmetric ceramic membranes are synthesized including several layers with different pore size distributions with the top-layer playing the main separation role. Titania has several properties such as photocatalytic activity and chemical stability making it sutitable as an option for the top-layer. This study is devoted to the preparation and characterization of a ceramic membrane, dip-coating of mesoporous interlayers and preparation of a microporous anatase top-layer via sol-gel technique. Moreover, the performance of the membrane modified by nano-copperis investigated for salt rejection enhancement. Membranes were characterized by FE-SEM and X-ray diffraction. The sol particle size was determined using DLS. Cross-flow filtration setup was used for membrane permeability and salt retention experiments. Membrane top-layer showed crystal structures including rutile and anatase phases. By increasing salt concentration, chloride rejection is decreased and retention is increased by increasing the pressure. In case of modified membranes using nano-copper, higher retentions are observed, with 35% rejection for NaCl and 73% for Na_2SO_4.

Keywords: *Ceramic membrane; Nanofiltration; Sol-gel; Dip-Coating*

How to cite this article

Shokri Doodeji M, Zerafat MM, Nejadian O. Fabrication and Charge Modification of Ceramic Membranes Using Copper Nanoparticles for Desalination. J. Nanoanalysis., 2017; 4(3): 247-254. DOI: 10.22034/jna.2017.542977.1027

INTRODUCTION

Droughts, world population and increased agricultural water consumption have led to the reduction of sweet water resources. During recent decades, various techniques are examined and developed to produce potable water from saline resources which comprise the highest portion of available water in the seas and oceans. Among these, membrane-desalination have been very much developed due to low temperature and low energy consumption. Polymeric membranes have many advantages, such as easy film forming characteristics, selectivity of chemical species and relatively inexpensive constituents. However, inorganic membranes are currently competing with their polymeric counterparts commercially. Inorganic membranes are resistant to chemical attack, have good mechanical strength and a high pH and oxidation resistance [1]. Inorganic membranes composed of metal oxide ceramics are gaining a common place in the market due to their

* *Corresponding Author Email: mmzerafat@shirazu.ac.ir*
Tel: +98 (917)3100957

high durability in water purification applications [2]. In harsh environments, only inorganic membranes offer the favorable requirements, however not used extensively due to the high cost and relatively poor control on pore size distribution during synthesis [3].

Nanofiltration with a low energy consumption compared to reverse osmosis can be a good alternative for desalination as a pressure-driven separation process rejecting very small moieties due to relatively high charge and pores < 2 nm [4]. Some of the most prevalent materials for ceramic membranes are α-alumina, γ-alumina [3,5], Zirconia [6] and titania [7]. Ceramic Substrates are used to provide the mechanical support by slip casting, dry-pressing and extrusion [8,9]. Van Gestel et. al (2002) used dry-pressing to prepare the substrate by sintering at 1300°C [10]. Khalili et. al (2015) prepared alumina substrates using two different additives for sintering. The results showed that the support made by ethanol had a more uniform and regular granulation and the support made from PVA had a narrower PSD and lower porosity [11].

Sol-gel is one of the most important techniques for preparation of ceramic membranes with advantages such as good control over pore size. Lennars et. al (1985) used sol-gel technique to develop ceramic ultrafiltration membranes for the first time [12]. Schaep et. al (1998) produced mesoporous γ-Al_2O_3 membranes by sol-gel dip-coating followed by thermal treatment. Various sintering temperatures were applied, leading to membranes with an average pore diameter ranging from 3.4 to 8.7 nm [13]. Van Gestel et. al (2002) prepared macroporous supports from α-Al2O3. Three types of colloidal sol-gel derived mesoporous interlayers are considered: Al_2O_3, TiO_2 and mixed Al_2O_3–TiO_2. The active NF top-layer is also very thin and fine-textured TiO_2. Different crystallographic properties of various membrane layers result in considerably different chemical stabilities [10]. Based on Tim Van Gestel et. al (2002), meseporous membranes are obtained by preparing a sol with larger particles which is possible using a water to precurser molar ratio>1. For smaller pores, the reverse is correct.

Pontalier et. al (1997) showed that membrane MWCO, determines the solute transfer either by diffusion or a combination of diffusion and convection. So, for the 100 Da membrane, diffusion was the dominant transfer mechanism for neutral and electrolyte solutions. Solute flux for all molecules were almost constant with>95% rejection values. When MWCO shifts from 100 to 400 Da, convection becomes prevalent. As a result, molecule segregation depends on the composition of the solution and ionic strength and solute Mw. It was shown that for neutral solutes such as glucose and lactose, sieving effect was dominant [14]. For electrolyte solutions, depending on the ionic radius, separation can be attributed to two mechanisms. The transfer of small ions is mainly convective since they can penetrate the pores. However, their transport along the pores is influenced by friction and electrostatic forces. Solute flux is therefore lower than solvent flux, particularly at low transmembrane pressures, leading to variation of rejection rate.

Also, Donnan effect plays a determining role in the separation of charge molecules. Transport of large ions with a high charge density is mainly diffusive. However, the effect of electrostatic forces is not negligible since molecules are repelled by the membrane surface; thus hindering diffusion. This indicates that for a dense membrane (MWCO<100 Da), mass transfer occurs mainly through a diffusive route. For membranes with higher MWCO (i.e.>100 Da), diffusive and convective transport mechanisms coexist, which can be used to model nanofiltration process [14].

Van Gestel et. al (2002) carried out zeta potential measurements as a function of pH to investigate the correlation between salt retention and charge of a ceramic membrane. Zeta potential measurements showed that the highly amphoteric character of the ceramic membrane, highly influences the salt retention. In the presence of mono-valent salts (NaCl, KCl, LiCl), a clear pH dependency of salt retention were observed. Infiltration tests as a function of ionic concentration and transmembrane pressure, the membrane shows a standard behavior as reported previously for conventional NF membranes. In contrast, for salts containing divalent ions (Na_2SO_4, $CaCl_2$), the commonly used exclusion rules based on Donnan theory lose their validity. In either case, zeta potential experiments indicated that a modified membrane charge is established due to selective ion adsorption. Based on the results,

the experimentally determined zeta potential is the key parameter for qualitative analysis of salt retention [15]. Tsuru et. al (2001) prepared titanium membranes by sol-gel process and results show that rejection is minimized around the isoelectric point (IEP). Higher rejections were obtained for the filtration of electrolytes with divalent co-ions, while low rejections were observed for electrolytes with divalent counterions. On the other hand, permeate volumetric flux was maximized near IEP and the fluxes were almost unchanged irrespective of the electrolyte type. However, permeate volumetric fluxes were decreased at pH>IEP. Dependency was pronounced for divalent counterions and smaller pore diameters, probably due to higher hydrodynamic resistance by ionically-adsorbed counter-ions [16]. Schaep et. al (1999) showed that salt retention was very much dependent on the solution pH due to the amphoteric character of such membranes. Minimal salt retention was found at the IEP (pH=7.5). Experiments were carried out with NaCl, $MgCl_2$ and $LaCl_3$ at various concentrations for both single salts and mixtures. Such a membrane has an amphoteric character, which allows to control the sign and value of charge density through pH control [13].

Exclusion due to membrane charge is considered as one of the main separation mechanisms occurring in charged membranes, which can be varied through various approaches to affect membrane rejection. Ghaee et. al (2016) fabricated thin-film composite (TFC) polyamide (PA) membranes by interfacial polymerization of m-phenylenediamine (m-PDA) and 2,4-diaminobenzene sulfonic acid with trimesoyl chloride (TMC) on a polysulfone sub-layer. In order to improve membrane permeability, zeolite was introduced into the thin film structure. Increased rejection of nitrate from 63% to 85% is attributed to surface charge enhancement. TFN permeability was almost doubled by the addition of nanozeolite [17]. Foorginezhad and Zerafat (2017) prepared microfiltration membranes from nano-clay. The membrane had negative charge at pH=6, suggesting adsorption of cationic dyes as the removal mechanism [18].

In this study, nanofiltration membranes are prepared using sol-gel dip-coating for investigation of charge modification by copper nano-particles, based on our previous studies on alumina-titania membranes prepared for desalination [11]. This study is devoted to investigating the effect of copper nanoparticles in order to modify surface charge for the desalination regarding flux and rejection of inorganic salts. The results show that modification of surface charge can bring about improvements in salt rejection.

EXPERIMENTAL

Materials

α-Alumina (AKP3000) was purchased from Sumitomo Chemical (Japan). Polyvinyl alcohol (Mw=72000 g/mol), nitric acid (65%), hydrochloric acid, titanium Isopropoxide and ethanol were purchased from Merck Co. used as received. Copper(II) chloride was obtained from Sigma Aldrich. Aluminum-tri-sec-butoxide was purchased from Sigma Aldrich. Deionized water is used throughout the experiments for preparation of all solutions.

Methods

The main apparatus used in the experiments include an ultrasonic cleaning device, Dynamic Light Scattering (Malvern-ZEN 3600), UV-Visible spectrophotometer (Perklin Elmer-Lambda35), FE-SEM (Mira3 Tescan-XMU), SEM (Wega 3 Tescan), Energy Dispersive X- ray Spectroscopy (ESD) and Sepahan Irman Tech dip-coater (Iran).

Support Preparation

The substrate is prepared via dry casting. A proper amount of alumina powder is mixed with a 7 wt% PVA solution. The suspension is pressed in the desired template, then sintered at 1250°C for 2 h [3,4].

Preparation of the intermediate layer

Membranes were prepared by conventional dip-coating. 1 mol of aluminum tri-sec-butoxide (ASB) was dissolved in 2 lit (L) deionized water and stirred at 8°C for 1 h. 0.07 mol HNO_3 per mol ABS was added to the sol. The mixture was stirred at 90°C for 2 h to remove butanol from the sol, and then put under reflux for 16-24 h and 2 h before the end, PVA solution (3.5 gr to 100 ml deionized water) was added to the mixture. The outer surface of the ceramic support was polished with 600 mesh sandpaper and washed several times with deionized water under ultrasonication and dried in the atmosphere. Afterwards, the ceramic support

was dip-coated and heat treated at 650-800°C for 3 h (heating rate 30°C/hr) to sinter the intermediate layer [11].

Preparation of the top-layers

In order to prepare the titania top-layer, 14.7 ml of titanium isopropoxide (TTIP) was added to 5 ml ethanol at room temperature and after 30 min, 100 ml water was added to induce hydrolysis. Afterwards, the solution was stirred at 90°C for 3 h while 1.3 ml HCl was added. The sol was put under reflux for 9 h. The modified membrane with the intermediate layer was washed with acetone and dried in the atmosphere, then coated with titania gel to form the top-layer using two-step dip-coating. The membrane was dried at 30°C over night and heat treated at 450c for sintering and calcination.

For the preparation of copper-modified membranes, an extra step is added after sol formation. Proper amounts of $CuSO_4.5H_2O$ are dissolved in the sol after reflux and HCl is added to the sol dropwise during dip-coating resulting in the preipitation and doping of Copper in the gel matrix.

Characterization

Surface and cross-section morphologies of the substrate and nanofiltration membrane were observed using FE-SEM and SEM. This can be combined with energy-dispersive X-ray spectroscope (EDS) to provide information on size, shape, structure and chemical composition. Energy-dispersive spectrometer (EDS) allows the determination of elements present in the membrane employed for the characterization of nanoparticles dispersion. Effective particle sizes in sols were measured by dynamic light scattering (DLS) using Invasive Back Scatter (NIBS) (INBS) technique. Also, M3-PALS method is used to determine Zeta-potential by DLS. Crystallite structure of support and nano-ceramic membranes were characterized using an X-ray diffractometer (Bruker AXS-D8 Advance).

Permeability

A dead-end cell was used to measure the membrane pure water flux. At steady state, pure water flux is defined as:

$$PWF = Q/(A\times t) \quad (1)$$

Where, Q is the volume of the permeated pure water (L), A is the effective area of the membrane (m^2), and is the permeation time (h) [19].

Feed and permeate salt concentrations were measured using an electric conductivity meter (Ecomet conductivity meter C65) in order to calculate salt rejection as follows:

$$R = (Cs-Cd)/Cs\times 100\% \quad (2)$$

Where, C_s and C_d denote the salt concentrations of feed and permeate [20].

Porosity and pore size

Porosity was determined by gravimetric method, defined as:

$$\varepsilon = (m_1-m_2)/(A\times l\times \rho_w) \quad (3)$$

Where, m_1 is the weight of wet membrane; m_2 is the weight of dry membrane; ρ_w is water density (0.998 g cm^{-3})(0.998 g/cm^{-3}); A is effective area of the membrane (m_2) and l is membrane thickness (m) [19].

Mean pore radius was determined by filtration velocity method. According to Guerout–Elford–Ferry equation, r_m can be calculated:

$$r_m = \sqrt{(((2.9-1.75\,\varepsilon)\times 8\eta hQ)/\varepsilon AP)} \quad (4)$$

Where, η is water viscosity; h the membrane thickness; Q the flux per unit time; P the operational pressure (0.1 MPa) and A the effective membrane area [21].

RESULT AND DISCUSSION

Porosity and pore size

Table 1 shows the porosity and pore size of the alumina support and alumina support with inter-layer determined by Eq.s 3 and 4.

Table 1. Porosity and pore size of alumina support and support with inter-layer

Membrane	Porosity (%)	Pore Size (nm)
Alumina substrate	34	320

Membrane morphology

Fig. 1 shows the FE-SEM image of the alumina substrate. The results show a dense and uniform structure without cracks.

FE-SEM micrograph of the membrane with intermediate layer is given in Fig. 2 which confirms coating of Al_2O_3 interlayer on the substrate surface with different magnifications.

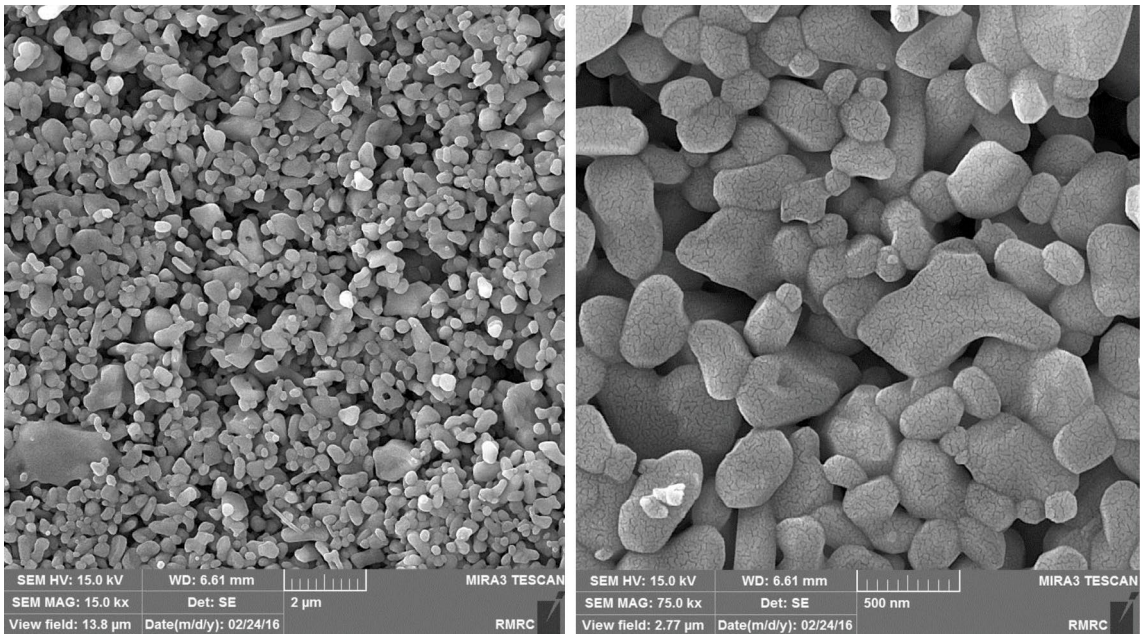

Fig. 1. The FE-SEM images of alumina support.

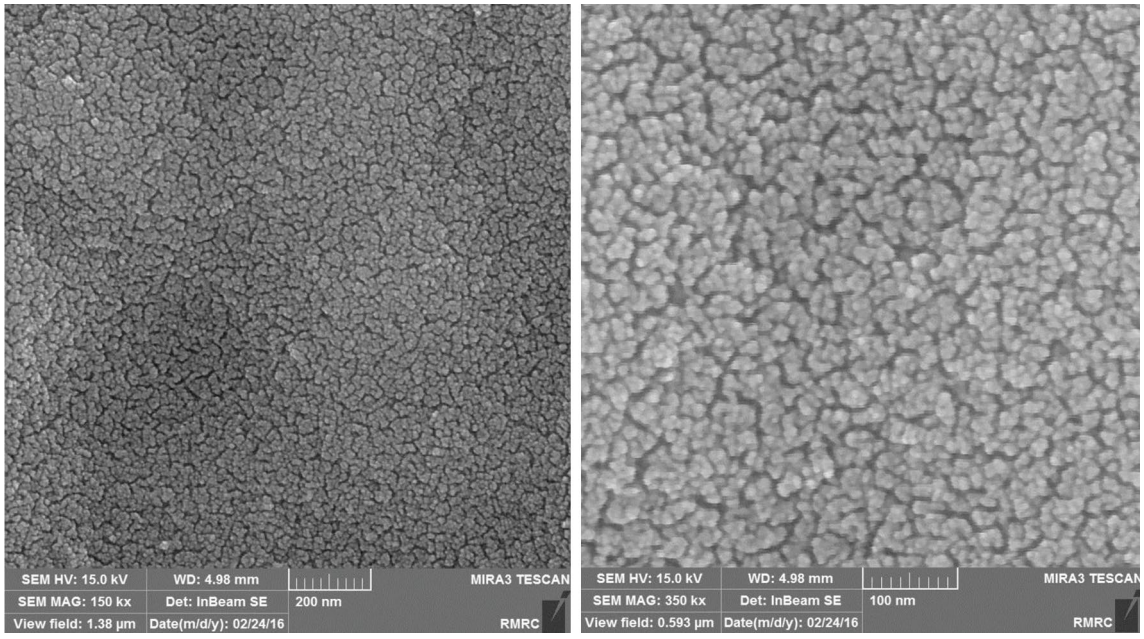

Fig. 2. FE-SEM image of the membrane surface in the intermediate alumina layer.

The FE-SEM images of the support coated top-layer are shown in Fig.3. This membrane is prepared using two-step dip-coating including the SEM image of the nano-membrane cross-section.

XRD Spectrum

X-ray diffraction (XRD) patterns were recorded over a 2Θ=10–90° range using a Bruker AXS-D8 Advance diffractometer. Fig. 4 shows the XRD pattern for the aluminia support. Sharp peaks approve the crystalline structure and for the sintering temperature of 1250°C, α-alumina and γ-alumina phases are observed.

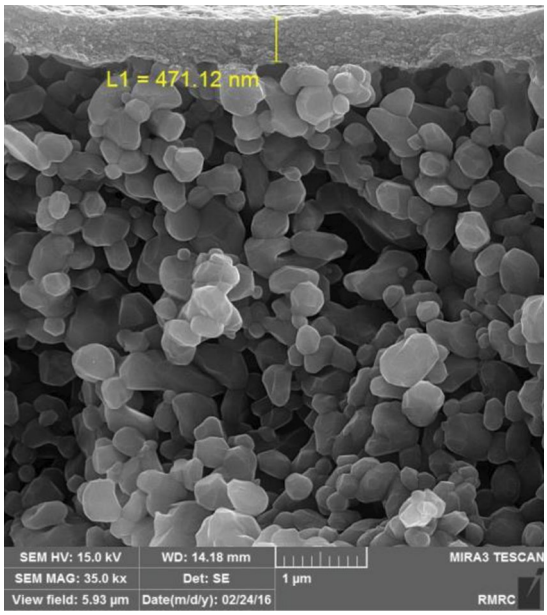

Fig. 3. FE-SEM image of TiO_2-2Cu membrane.

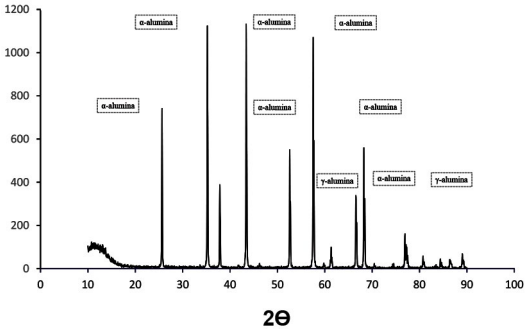

Fig. 4. XRD pattern of the substrate.

Fig. 5 shows the XRD pattern for the calcined nano-ceramic membrane at 450°C. Different crystalline structures are identified in the XRD pattern as: the rutile and anatase phase for TiO_2 and the cubic phase for Al_2O_3.

PSA analysis of the Bohemite Sol

Particle size is an important factor on the roughness and pore size. Inter layer particle size analysis of bohemite sol is performed using DLS Analysis. Fig. 6 shows that the maximum number of particles have a narrower size distribution under 42 nm with an 29.93 nm average value.

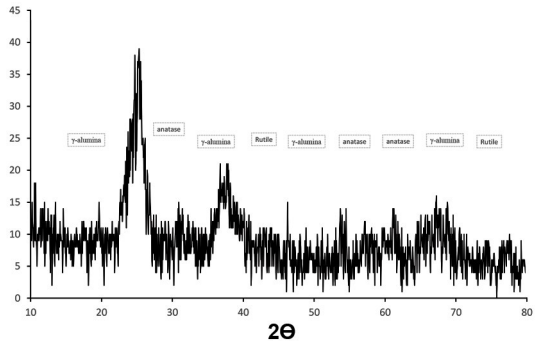

Fig. 5. The XRD pattern of the multilayer membrane.

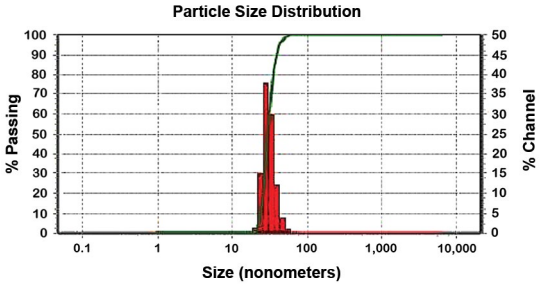

Fig. 6. Particle size distribution of the bohemite Sol.

Feed concentration

Salt concentration can influence the rejection performance of hybrid membranes [22]. The main purpose of this study is to investigate the effect of feed concentration on the rejection for single salt NaCl and Na_2SO_4 solutions. Na_2SO_4 and NaCl are used to investigated the separation under 6 bar and pH=8. Table 2 shows various membranes with their corresponding rejection values at 6 bar with different Cu nanoparticle wt. %.

Fig. 7 shows Na_2SO_4 rejection for nano-ceramic membrane (TiO_2) and modified nano-ceramic membranes (TiO_2-1Cu & TiO_2-2Cu). By increasing salt concentration, rejection is decreased due to the enhancement of ionic strength and reduction of electrical double layer thickness. Adding copper nanoparticles to the membrane surface lead to the enhancement of rejection as a result of improvement of Donnan effect which reflects itself in the enhancement of zeta potential improvement from 147.86 to -170.93.

Table 2. Pure water flux and rejection at 6 bar

Membrane	Cu nanoparticles (wt.%)	Pure water flux ($L.m^{-2}h^{-1}$)	Na_2SO_4 Rejection (%)	NaCl Rejection (%)
Substrate	-	98	-	-
TiO_2	-	10.5	55.6	28.6
TiO_2-1Cu	10	9.8	70.3	35.3
TiO_2-2Cu	20	9.5	73	35.6

Fig. 8 shows membrane rejection for NaCl. Similar to Na_2SO_4, increasing feed concentration leads to increasing ionic strength that results in the reduction of salt rejection.

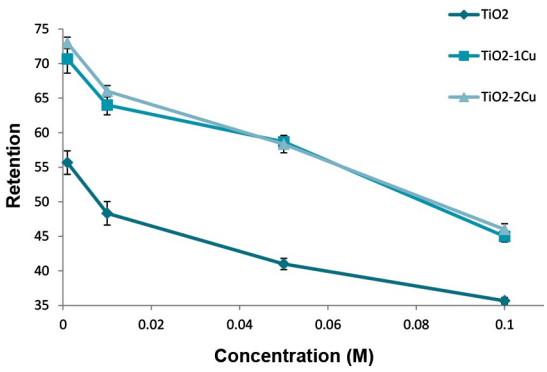

Fig. 7. Effect of feed concentration on Na_2SO_4 rejection at 7 bar.

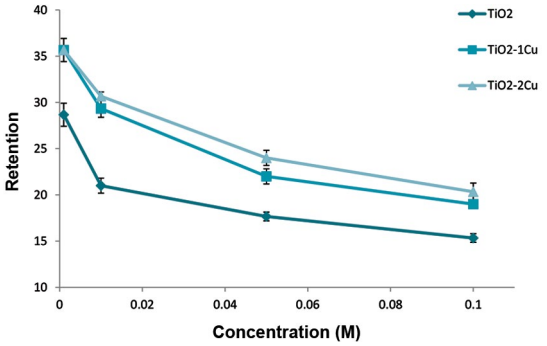

Fig. 8. Effect of feed concentration on NaCl rejection at 6 bar.

Figs. 7 and 8 show the rejection of Na_2SO_4 and NaCl increasing from 55 to 73 and 28 to 35 for membranes modified with nanoparticles. This salt rejection enhancement can be due to the increased surface charge on the ceramic membranes [9]. Based on the results, Na_2SO_4 rejection is higher compared with NaCl at the same concentration which can be attributed to the larger ionic radius of SO_4^{2-}.

Fig. 9 shows Na_2SO_4 and NaCl rejection at various operating pressures. Based on the results, rejection is primarily enhanced and reaches a constant value which is expected to lessen slightly by increasing the pressure.

Actually, concentration gradient, pressure gradient and electric charge gradient are three important factors in ionic transport through membrane pores. At low pressures, diffusion has a significant impact on rejection which limits the rejection. While at higher pressures, convection is grown which results in the enhancement of rejection.

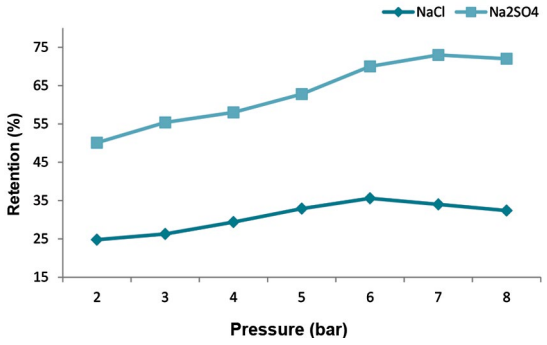

Fig. 9. The variations of rejection for the modified membrane TiO_2-2Cu as a function pressure.

EDS analysis

Fig. 10 shows the EDS result of the modified nano-ceramic membrane with Cu that approves

the existence of Cu nano-particles in the top-layer structure.

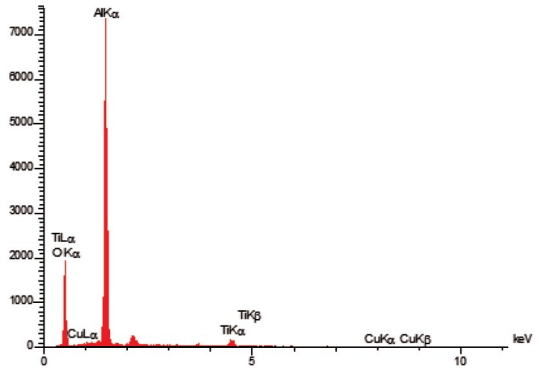

Fig. 10. The EDS of the TiO_2-2Cu membrane top layer (top-layer).

Also, Table 3 shows weight percent and atomic percent of the elements present in the top-layer.

Table 3. Weight and atomic percent of elements in top-layer

Element	weight percent (wt%)	Atomic Percent (mm/s)
Aluminum	6.83	4.43
Titanium	8.38	3.06
Copper	0.43	0.12
Oxygen	84.37	92.37

CONCLUSION

In this study, nano-ceramic membranes were fabricated using sol-gel technique for investigating the effect of charge modification on desalination performance. Low-cost ceramic supports were prepared using α-alumina powder as raw material for water desalination. The effect of Cu nanoparticles was also studied. The results of FE-SEM and XRD analyses indicate TiO_2 coating on the support. The results show that the membrane with 20 wt. % nano-copper has the best performance. 35% rejection for NaCl and 73% rejection for Na_2SO_4 were obtained using the as-fabricated membranes at optimal conditions.

CONFLICT OF INTEREST

The authors declare that there are no conflicts of interest regarding the publication of this manuscript.

ACKNOWLEDGMENT

Thanks to Iran National Science Foundation (INSF) for financial support of the project.

REFERENCES

1. C. Labbez, P. Fievet, A. Szymczyk, A. Vidonne, A. Foissy and J. Pagetti, J. Memb. Sci., 208, 315 (2002).
2. J. M. Skluzacek, M. I. Tejedor and M. A. Anderson, J. Memb. Sci., 289 , 32 (2007).
3. M. Khalili, S. Sabbaghi, M. M. Zerafat and H. Daneshmand, Int. J. Nano Dimens., 5, 393 (2014).
4. M.H. Yousefi, M.M. Zerafat, M. Shokri Doodeji and S. Sabbaghi, J. water Environ. Nanotechnol. (in press) (2017).
5. M. A. Anderson, M. J. Gieselmann and Q. Xu, J. Memb. Sci., 39, 243 (1988).
6. H. Qi, G. Zhu, L. Li and N. Xu, J. Sol-Gel Sci. Technol., 62, 208 (2012).
7. S. M. Doke and G. D. Yadav, Chem. Eng. J., 225, 483 (2014).
8. S. Sarkar, Trans. Indian Ceram. Soc., 73, 239 (2014)
9. T. Van Gestel, H. Kruidhof, D. H. A. Blank and H. J. M. Bouwmeester, J. Memb. Sci., 284, 128 (2006).
10. T. Van Gestel, C. Vandecasteele, A. Buekenhoudt, C. Dotremont, J. Luyten, R. Leysen, B. Van der Bruggen and G. Maes, J. Memb. Sci., 207, 73 (2002).
11. M. Khalili, S. Sabbaghi and M. M. Zerafat, Chem. Pap., 69, 309 (2015)
12. A. F. M. Leenaars and A. J. Burggraaf, J. Memb. Sci., 24, 261 (1985).
13. J. Schaep, C. Vandecasteele, B. Peeters, J. Luyten, C. Dotremont and D. Roels, J. Memb. Sci., 163, 229 (199)
14. M.M. Zerafat, M. Shariati-Niassar, S.J. Hashemi, S. Sabbaghi, A.F. Ismail and T. Matsuura, Desalination, 320, 17 (2013).
15. T. Van Gestel, C. Vandecasteele, A. Buekenhoudt, C. Dotremont, J. Luyten, R. Leysen, B. Van Der Bruggen and G. Maes, J. Memb. Sci., 209, 379 (2002).
16. T. Tsuru, D. Hironaka, T. Yoshioka and M. Asaeda, Sep. Purif. Technol., 25, 307 (2001).
17. A. Ghaee, M. M. Zerafat, P. Askari, S. Sabbaghi and B. Sadatnia, Environ. Technol., 38, 772 (2017).
18. S. Foorginezhad and M. M. Zerafat, Ceram. Int., 43, 15146 (2017).
19. J.F. Li, Z.L. Xu, H. Yang, L.Y. Yu and M. Liu, Appl. Surf. Sci., 255, 4725 (2009).
20. N. A. A. Hamid, A. F. Ismail, T. Matsuura, A. W. Zularisam, W. J. Lau, E. Yuliwati and M. S. Abdullah, Desalination, 273, 85 (2011).
21. C. Feng, B. Shi, G. Li and Y. Wu, J. Memb. Sci., 237, 15 (2004).
22. Z. Chen, F. Chen, F. Zeng and J. Li, Desalination, 349, 106 (2014).